Surface modes in accumulation layers

A. Puri* and W. L. Schaich
Physics Department and Materials Research Institute, Indiana University, Bloomington, Indiana 47405
(Received 3 May 1984; revised manuscript received 17 September 1984)

We study the coupled modes of plasmons and optical phonons near a surface accumulation layer on an ionic semiconductor. Using a simple model geometry the number, dispersion, and external electronic coupling of surface collective modes are described. Several model calculations are presented to illustrate these properties. Various limiting cases allow comparison with earlier work. We identify the analogs within our model of plasmarons and subband excitations. A new set of surface modes is described, whose frequencies lie in the phonon range but whose existence requires spatial dispersion in the plasmon response. Their observation in electron-energy-loss spectra should be possible.

I. INTRODUCTION

In a recent paper[1] one of us presented a hydrodynamic model calculation of electron-energy-loss spectra (EELS) which agreed reasonably well with experimental data from a doped GaAs surface.[2,3] In this analysis the approximation of a uniform density of charge carriers was used since band bending is not thought to be significant over the probing depth of the electron beam.[4] One can imagine, however, systems in which the opposite limit is more appropriate, i.e., that the charge carriers are localized much closer to the surface than the probing depth. We have in mind particularly an electron accumulation layer on ZnO, for which EELS data already exist.[5–8]

In this paper we examine the qualitative effects of such a confined carrier density on the existence, dispersion, and external electronic coupling of surface collective modes involving plasmons and optical phonons. There has been a large amount of previous theoretical work in this general area involving models both more and less sophisticated than the ones we shall treat.[9,10] One of our goals in fact is to study a tractable model in which by varying parameters different physical effects can be exhibited and various theories compared. We shall emphasize comparisons with the theoretical approach of Gersten,[11,12] which is quite different from ours but which has been successful in interpreting the EELS data from ZnO.[5–8]

All of the calculations contain both electrons and phonons. Our focus will be on the effects of changes in the electronic properties, specifically in their distribution and spatial dispersion. The geometry of the system is chosen to be simply three homogeneous regions: vacuum on one side, an ionic semiconductor on the other, and in between a layer of width d of the same semiconductor containing a uniform, equilibrium density of electrons, n_0.

The response of the system will be determined from various postulated dielectric constants and hydrodynamic equations. The effect of the optical phonons will always be treated via a local dielectric constant, which at frequency ω is

$$\epsilon_{\rm ph}(\omega)=\epsilon_\infty\frac{\omega_L^2-\omega^2-i\omega\gamma}{\omega_T^2-\omega^2-i\omega\gamma}\ , \tag{1}$$

where ω_L (ω_T) is the longitudinal (transverse) optical-phonon frequency and γ is a decay rate. The electrons' response will be computed from a hydrodynamic equation:

$$\frac{\partial\vec{\rm j}}{\partial t}=\frac{\omega_p^2}{4\pi}\vec{\rm E}-\beta^2\vec{\nabla}\delta\rho-\frac{\vec{\rm j}}{\tau}\ , \tag{2}$$

where $\vec{\rm E}$ is the total electric field, $\vec{\rm j}$ ($\delta\rho$) is the induced electron current (charge) density, ω_p is the (unscreened) plasma frequency, β is the spatial dispersion parameter, and $1/\tau$ is another decay rate. Combining the above constitutive relations with Maxwell's equations leads to the dispersion relations of various surface excitations. Note that our approach takes no account of the possible size quantization of the carriers in the middle layer. The resulting theory is easy to develop and interpret, and can be readily applied to the existing EELS data. Limiting ourselves to this particular application, we can omit retardation effects.

When β is zero, one has a completely local theory. This case is treated in Sec. II, where both the surface mode dispersion relations and their external electronic coupling are determined. The plasmarons studied by Gersten[11,12] are present already at this level. In Sec. III we allow β to be finite which makes the response spatially nonlocal. The dispersion and coupling constants of the modes found earlier are in general only slightly changed but a host of new surface modes appear due to longitudinal waves trapped in the accumulation layer. The trapped modes that lie near plasma frequencies may be interpreted as the analogs in our classical model of subband excitations. There are also trapped modes near the phonon frequencies, which is a new feature that we have discovered. The influence of these modes on the EELS spectral function is illustrated. Finally, in an appendix we discuss how the parameters of our model may be estimated.

II. LOCAL THEORY

Neglecting retardation reduces Maxwell's electrodynamic equations to those of electrostatics. We may then describe the electric field $\vec{\rm E}$ solely in terms of a scalar potential Φ as $\vec{\rm E}=-\vec{\nabla}\Phi$. We denote the variable

along the interface normal x, with $x=0$ at the vacuum-layer interface and $x=d$ at the layer-semiconductor interface. In the local limit the response is fully determined by the dielectric function

$$\epsilon(\omega,x)=\begin{cases}\epsilon_0=1, & x<0\\ \epsilon_1=\epsilon_{\rm ph}(\omega)-\dfrac{\omega_p^2}{\omega^2+i\omega/\tau}, & 0<x<d\\ \epsilon_2=\epsilon_{\rm ph}(\omega), & d<x\end{cases} \tag{3}$$

where the subscripts 0, 1, and 2, refer to the vacuum, layer, and semiconductor media, respectively; $\epsilon_{\rm ph}$ is given by (1); and $\omega_p^2=4\pi n_0 e^2/m^*$, with m^* the effective mass of an electron and e its charge. Since by assumption the media have translational invariance parallel to the interface, the system's linear response preserves from any applied perturbation both $\bar{Q}$, the two-dimensional wave vector parallel to the surface, and ω, the frequency. Assuming that the only induced charge resides at the interfaces, we can write the space-time variation of Φ in the presence of an external perturbation as a sum of partial waves, each with the good quantum numbers $\bar{Q}$ and ω:[13]

$$\Phi(\vec{x},t)=e^{i(\bar{Q}\cdot\bar{X}-\omega t)}\times\begin{cases}e^{-Qx}+\lambda e^{Qx}, & x<0\\ \alpha_+ e^{Q(x-d)}+\alpha_- e^{-Qx}, & 0<x<d\\ \alpha e^{-Q(x-d)}, & d<x.\end{cases} \tag{4}$$

The e^{-Qx} represents the (unit) external perturbation and the other partial waves describe the system's linear response. The matching coefficients λ, $\alpha_\pm$, and α are to be determined by requiring at each interface continuity of both the parallel components of $\vec{E}$ and the normal component of $\vec{D}=\epsilon\vec{E}$.

Consider in particular $\lambda(\bar{Q},\omega)$, which controls the response produced in the vacuum. For electron loss spectroscopy the differential scattering probability can with the neglect of impact scattering and the use of semiclassical arguments be written as[14]

$$P(\bar{Q},\omega)=\frac{2e^2}{\pi^2\hbar Q}\left[\frac{Qv}{Q^2v^2+(\bar{Q}\cdot\bar{V}-\omega)^2}\right]^2{\rm Im}[-\lambda(\bar{Q},\omega)]\,, \tag{5}$$

where Im denotes "imaginary part of" and the velocity (normal component v, parallel component $\bar{V}$) describes the incoming external electron which will lose energy $\hbar\omega$ and parallel momentum $\hbar\bar{Q}$ in scattering (nearly) specularly from the surface. The coefficient λ diverges at the surface modes,[15] which in the absence of damping, $\gamma=0=1/\tau$, occur at real Q and ω. The locations of these divergences follow from the four matching equations, which reduce to the requirement

$$\frac{\epsilon_1+\epsilon_2}{\epsilon_1-\epsilon_2}\frac{\epsilon_1+\epsilon_0}{\epsilon_1-\epsilon_0}=e^{-2Qd}\,. \tag{6}$$

With the ϵ of (3), there are at each Q four solutions of (6) for ω^2.

Before presenting a numerical calculation of these roots we examine several limiting cases where the physics is more transparent.

A. $Qd\to\infty$

We view this case as the limit of a very thick accumulation layer. Equation (6) reduces to

$$(\epsilon_1+\epsilon_2)(\epsilon_1+\epsilon_0)=0\,. \tag{7}$$

We interpret the solution of $\epsilon_1+\epsilon_0=0$ as the surface modes for an isolated vacuum—accumulation-layer system. For our choice of ϵ there are two such modes, called $\omega_1(\infty)$ and $\omega_3(\infty)$, associated with plasmons and phonons. Similarly we interpret the solution of $\epsilon_1+\epsilon_2=0$ as the interface modes for an isolated accumulation-layer—semiconductor system. Again there are two such modes, now called $\omega_2(\infty)$ and $\omega_4(\infty)$. For our choice of parameters, which has the plasma frequency larger than phonon frequencies, $\omega_1>\omega_2>\omega_3>\omega_4$, and for large Qd, ω_1 and ω_2 have plasmon frequencies while ω_3 and ω_4 have phonon frequencies.

B. $Qd\to 0$

There are several ways to interpret this limit and hence several subcases to consider. For the easiest we imagine that $d\to 0$ at fixed Q and n_0. This amounts to removing the accumulation layer completely and leaving only the single surface mode of a vacuum-semiconductor system: $\epsilon_0+\epsilon_2=0$. An alternate viewpoint that preserves four solutions allows $Q\to 0$ at fixed d. Now it is physically appropriate to use as ways of satisfying (6), when $Qd=0$, any of the following:

$$\epsilon_0+\epsilon_2=0\,, \tag{8a}$$

$$\epsilon_1=0\,, \tag{8b}$$

$$\epsilon_1=\infty,\ \text{but } \epsilon_2 \text{ and } \epsilon_0 \text{ finite}\,. \tag{8c}$$

We have already interpreted the single solution of Eq. (8a), which we call $\omega_2(0)$. Equation (8b) has two roots, one associated with "bulk" plasmons and one with bulk phonons within an isolated accumulation layer. We call them $\omega_1(0)$ and $\omega_3(0)$. Lastly Eq. (8c) has for our choice of ϵ one solution: $\omega_4(0)=0$. Again our labeling scheme yields $\omega_1>\omega_2>\omega_3>\omega_4$, but now only ω is in the plasmon frequency range.

A third way to consider $Qd\to 0$ is to imagine at fixed Q, $d\to 0$ while $n_0\to\infty$ with $N=dn_0$ fixed. In this process the accumulation layer is shrunk to a charge sheet and (6) becomes

$$\epsilon_0+\epsilon_2=\frac{\omega_p^2 d}{\omega^2}Q\,, \tag{9}$$

where $\omega_p^2 d\to 4\pi Ne^2/m^*$, a constant. This equation has two solutions for ω^2 at each Q, one of which for small Q has $\omega\propto\sqrt{Q}$, the signature of the two-dimensional surface plasmon.[16–20]

Now we turn to a numerical solution of (6), using the model parameters employed by Gersten in his study of ZnO;[12] i.e., $\hbar\omega_T=50.7$ meV, $\hbar\omega_L=71.7$ meV, $\epsilon_\infty=4.0$,

and $m^*/m=0.25$. We show in Fig. 1(a) the surface mode dispersion relations for one choice of $N=dn_0$. Our prescription for separating N into d and n_0 is outlined in the Appendix. It yields for $N=4\times10^{13}/\text{cm}^2$ values of $d=15.6$ Å and $n_0=2.56\times10^{20}/\text{cm}^3$. Only the lowest three modes are shown in Fig. 1(a); $\omega_1(Q)$ lies well off scale since it runs between $\omega_1(0)=598$ meV and $\omega_1(\infty)=536$ meV. For both large and small Q, the limiting behavior discussed above helps one sort out the nature of the branches. When a $d\omega_i/dQ\to0$ at large Q, we find that $\omega_i(Q)$ has become $\omega_i(\infty)$. The $\omega\propto\sqrt{Q}$ behavior is exhibited (partially) by both branch 2 and 4, the former above ω_L and the latter below ω_T.

In Gersten's analysis of this same system a rather different formulation is used. The electronic motion in the x direction is considered in the extreme quantum limit and essentially frozen out. Instead of a driving force due to $\vec{E}$ at $\vec{x}$, what appears in his equations is the average over the ground-state electronic wave function of the parallel components of $\vec{E}$. Since the electrons are not allowed to come out of this ground state for motion normal to the layer, he has no subband excitations. In terms of our model this means that branch 1, the nearly pure, bulk plasmon of the accumulation layer is absent in his theory. Still the dispersion curves for the other modes appear quite similar to his, although it is worth remarking that our modes 3 and 4 here stay below ω_T, while his lowest two modes do rise to ω_L for large Q.

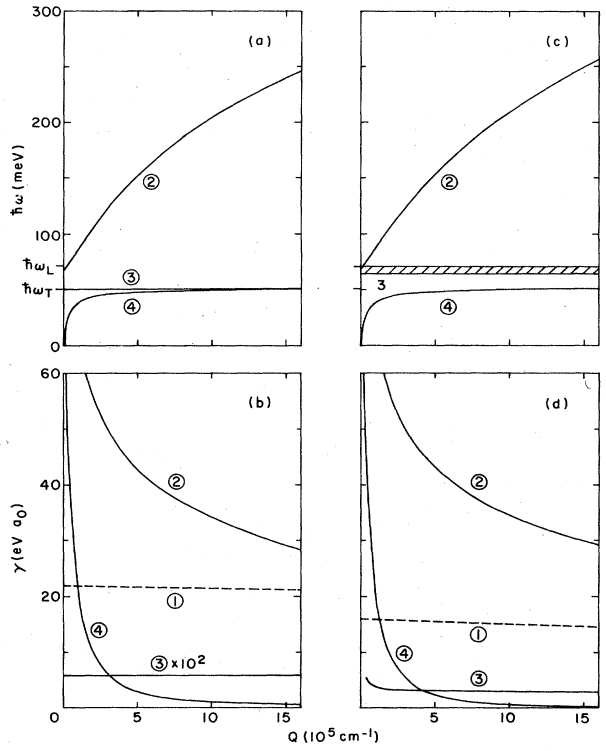

FIG. 1. Surface-wave dispersion and external coupling coefficients for $N=4\times10^{13}$ cm^2. In (a) and (b) the dispersion relations are shown on the same scale; in (c) and (d) the coupling constants are drawn on a common scale. The (a) and (c) panels have $\beta=0$, while the (b) and (d) panels have $\beta\neq0$. See text for specific parameter choices. Since the mode 1 lies off scale in (a) and (b), its γ_1 is denoted by a dashed line in (c) and (d). Also we have multiplied γ_3 by 10^2 to make it visible in (c). The shaded band above ω_3 in (b) contains an infinity of modes.

To make further comparisons with Gersten we need to find the analog of the coupling constants that he plots.[12] Such quantities appear in a second quantized expression of the surface mode Hamiltonian, $H=H_0+H_1$, where

$$H_0=\sum_{\bar{Q}}\sum_i \hbar\omega_i(\bar{Q})(a^\dagger_{\bar{Q},i}a_{\bar{Q},i}+\tfrac{1}{2}) \tag{10a}$$

and

$$H_1=\sum_{\bar{Q}}\sum_i \Gamma_{\bar{Q},i}e^{i\bar{Q}\cdot\bar{x}}e^{Qx}(a_{\bar{Q},i}+a^\dagger_{-\bar{Q},i}),\quad x<0\,. \tag{10b}$$

Here $a^\dagger_{\bar{Q},i}$ ($a_{\bar{Q},i}$) is a creation (annihilation) operator of the collective surface mode labeled by $\bar{Q}$ and i and the $\Gamma_{\bar{Q},i}$ are coupling constants to external electrons. Although Eq. (11) may be derived by standard methods from our eigenmodes and equations of motion, the resulting expressions are not very revealing so we present here only a numerical evaluation of the $\Gamma_{\bar{Q},i}$.

This is accomplished by comparing two alternate expressions for the differential scattering probability of (5). First note that in the absence of damping (5) becomes

$$P(\bar{Q},\omega)=\frac{2e^2}{\pi^2\hbar Q}\left[\frac{Qv}{Q^2v^2+(\bar{Q}\cdot\bar{V}-\omega)^2}\right]^2 \times\sum_i R_{\bar{Q},i}\delta(\omega-\omega_i(\bar{Q}))\,, \tag{11}$$

where the $R_{\bar{Q},i}$ are easily calculated once we locate the poles of λ on the real axis. A result formally equivalent to (11) may be found by using an external electron on a specular scattering trajectory to drive the Boson Hamiltonian (10) into excited states.[21] This yields

$$P(\bar{Q},\omega)=\frac{A}{(2\pi)^2}\frac{4e^2}{\hbar^2}\left[\frac{Qv}{Q^2v^2+(\bar{Q}\cdot\bar{V}-\omega)^2}\right]^2 \times\sum_i |\Gamma_{\bar{Q},i}|^2\delta(\omega-\omega_i(\bar{Q}))\,, \tag{12}$$

where A is the quantization area of the surface. Comparing (11) and (12) reveals that

$$A|\Gamma_{\bar{Q},i}|^2=2R_{\bar{Q},i}/Q \tag{13}$$

and we show in Fig. 1(b) our numerical results for the A independent quantities plotted by Gersten, $\gamma_{\bar{Q},i}=\sqrt{A}\,|\Gamma_{\bar{Q},i}|$. The relative size of the $\gamma_{\bar{Q},i}$ and their dependence on Q is roughly similar to that found by Gersten, except for our mode 3 which is too close to ω_T to yield a significant external coupling. However, when we allow finite spatial dispersion, this situation changes.

III. NONLOCAL THEORY

In this section we again determine the dispersion and external coupling of surface modes, but now with β finite

in Eq. (2). Note that this procedure places spatial dispersion into only the electronic response in the accumulation layer. Most of the modes we shall find would be unstable due to nonradiative decay into the semiconductor substrate if we were to include a low density of electrons with spatial dispersion there. This constraint has been noted by Crowne[22] and avoided by Das Sarma *et al.*,[23,24] who consider the surface to have a depressed electron density compared to that in the bulk (i.e., a surface depletion layer rather than accumulation layer). Most other theories of surface modes associated with surface layers of electrons have either allowed no electrons in the substrate, which we as well as Refs. 5—8, 11, 12, and 16—20 do; or have allowed no spatial dispersion there, as in Refs. 25—27.

When β is finite in the accumulation layer we must include in the partial wave expansion of Φ waves that are nonzero throughout $0<x<d$ under the operation ∇^2. This changes the middle line of Eq. (4) to[28]

$$\Phi(\vec{x},t)=e^{i(\vec{Q}\cdot\vec{X}-\omega t)}[\,\alpha_+e^{Q(x-d)}+\alpha_-e^{-Qx}+\alpha_s\sin(p_l x)+\alpha_c\cos(p_l x)]\,, \quad 0<x<d \tag{14}$$

where (with l for "longitudinal")

$$p_l^2=-Q^2+(\omega^2+i\omega/\tau-\omega_p^2/\epsilon_{\rm ph})/\beta^2 \tag{15}$$

and p_l is chosen to lie in the first quadrant of the complex plane. The two extra matching coefficients in (14) may be determined by imposing the additional boundary conditions (ABC), that the normal component of the electron current vanishes at $x=0$ and d. This is a common, but not unique, choice. It forbids any induced charge on the interfaces. An alternate ABC choice that we have advocated[1,13,28,29] produces in the present simple configuration no change from the $\beta=0$ results. The two matching equations from the ABC are to be combined with the four previous conditions for continuity at each interface of parallel $\vec{E}$ and normal $\vec{D}$, where now in the layer

$$\vec{D}=\epsilon_{\rm ph}\vec{E}+4\pi\vec{j}/(-i\omega)\,. \tag{16}$$

As in Sec. II we initially set the damping rates to zero and numerically locate the poles (and residues) of $\lambda(\bar{Q},\omega)$ for real Q and ω.

Our results for the same parameter choices (except $\beta\neq0$) as in Figs. 1(a) and 1(b) are shown in Figs. 1(c) and 1(d). The prescription for β is given in the Appendix; its value is fixed once m^* and n_0 are specified. The effect of finite β on the modes already present in Fig. 1(a) is not great. As $Q\to\infty$, ω_3 and ω_4 now tend to ω_L while ω_1 and ω_2 tend to infinity (as $\omega\sim\beta Q$). These changes bring the mode dispersions into good qualitative agreement with Gersten's results.[12]

However, the most striking change in the surface mode spectrum is not really apparent in Fig. 1(c). The system develops an infinity of bound modes both for $\omega_1\leq\omega<\infty$ [off the scale in Fig. 1(c)] and for $\omega_3\leq\omega<\omega_L$ [in the shaded region of Fig. 1(c)]. The first few of the latter set of modes are shown in the expanded Fig. 2. Such a spectrum does not occur in Gersten's model.

The physical origin of these additional bands of surface modes is the possibility of trapped longitudinal waves in the accumulation layer. They occur in regions where $p_l^2>0$ and are well described by the condition

$$p_l d=n\pi,\quad n=1,2,\ldots, \tag{17}$$

which allows us to label them as successive standing waves. For frequencies above ω_1 they may also be simply interpreted as plasmons of ever-decreasing wavelength. However, between ω_T and ω_L their interpretation is more subtle since the spatial dispersion responsible for the standing wave is an electronic effect while the mode frequency is that of phonons. Hence one might say that the electronic contribution comes from a virtual polarization of the plasmon fields, to which the phonons respond with negative screening ($\epsilon_{\rm ph}<0$). The point we emphasize is that these additional modes in the phonon range have a one-to-one correspondence with the discrete electronic excited states of the accumulation layer. Thus even when one uses better models of the accumulation layer, e.g., including single-particle as well as collective excitations, this correspondence should remain. For instance, subband excitations, which have been studied within the random-phase approximation,[30—32] should, when optical phonons are included, produce extra surface modes between ω_T and ω_L. These modes are in addition to the section of the two-dimensional plasmon that extends into the phonon band (i.e., ω_2 as $Q\to0$). This last point is illustrated in Fig. 2 where we show how ω_2 goes through a series of avoided crossings with the additional modes.

While on the subject of additional modes we mention that we did consider the suggestion that an anisotropic, but local, dielectric function can allow one to directly in-

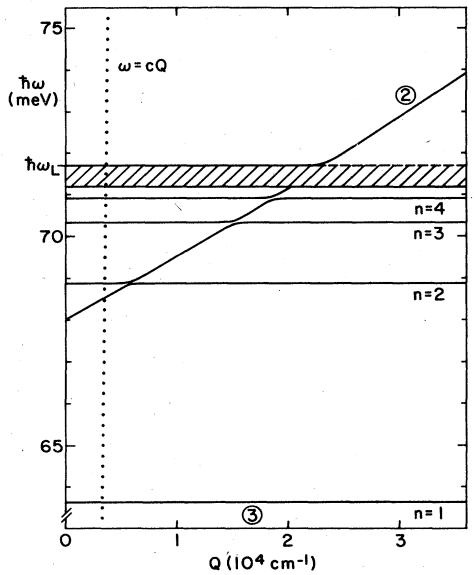

FIG. 2. Surface-wave dispersion for $\beta\neq0$. The same parameters are used as in Fig. 1(c) but both the ω and Q scales have been expanded so the first four of the standing-wave modes can be seen. The vacuum light line is shown by the dotted line. Retardation effects, which have been neglected here, become important near it.

clude subband excitations in the model.[33] In our notation, one would replace ϵ_1 in Eq. (3) (after setting $1/\tau=0=\gamma$) with

$$\epsilon_\perp=\epsilon_{\rm ph}(\omega)+\frac{\omega_p^2}{\omega_0^2-\omega^2} \tag{16'}$$

for the ratio between normal $\vec{D}$ and normal $\vec{E}$ and with

$$\epsilon_{||}=\epsilon_{\rm ph}(\omega)-\frac{\omega_p^2}{\omega^2} \tag{16''}$$

for the ratio of parallel $\vec{D}$ to parallel $\vec{E}$. Here ω_0 is the frequency of a single (bare) subband excitation. With such a dielectric function the form of the scalar potential within the layer is modified in the local limit from Eq. (4) to

$$\Phi(\vec{x},t)=e^{i(\vec{Q}\cdot\vec{X}-\omega t)}(\alpha'_+e^{Q'(x-d)}+\alpha'_-e^{-Q'x}),\quad 0<x<d \tag{18}$$

where the choice $Q'=Q(\epsilon_{||}/\epsilon_\perp)^{1/2}$ insures that $\vec{\nabla}\cdot\vec{D}=0$ inside the layer. This modification has little effect on the modes ω_2, ω_3, and ω_4 provided $\omega_0>\omega_1$, but two infinities of extra modes appear. These lie either below ω_T or above ω_L, i.e., in frequency regions where $\epsilon_{||}/\epsilon_\perp<0$ so in turn Q' is imaginary and standing waves can be established in the accumulation layer. We do not believe that these solutions have physical significance since they can have arbitrarily small wavelengths at no energy cost due to a lack of spatial dispersion in the model. Hence we pursue them no further.

Returning to our model with spatial dispersion we next discuss the coupling constants for the modes of Fig. 1(c). These are shown in Fig. 1(d) and were calculated from the prescription (13). The γ_1 is the coupling constant for the (lowest) $n=1$ standing plasmon wave; while (for $Q\geq 4\times 10^4$ cm^{-1})

$$\gamma_3=\left[\sum_{n=1}^{\infty}\gamma_{3,n}^2\right]^{1/2}, \tag{19}$$

which describes the net effect of the whole band of extra modes between ω_3 and ω_L. The sum in (19) converges to three-digit accuracy after 10—20 terms. Compared to Fig. 1(b), for which $\beta=0$, the most significant change is that γ_3 now has a comparable magnitude to the other γ_i's. Mathematically this occurs since the trapped modes are not too close to ω_T. In the same vein note that γ_4 vanishes when ω_4 crosses ω_T; it recovers to finite values at larger Q. This behavior is also evident in Gersten's figures. Indeed the qualitative agreement between our $\beta\neq 0$ dispersion curves and coupling constants and those of Gersten imply that our theory could be equally well fit to present experimental data.[5–8]

The differences between our surface mode spectra and those of Gersten have been purposely suppressed by the plotting scheme of Fig. 1 which, however, is appropriate at the current stage of experimental and theoretical knowledge. For ZnO there has been no report of additional losses just above the ω_2 mode, which produces the dominant peak in EELS. Thus there is no experimental evidence yet for subband excitations or our ω_1 bulk plasmon mode. Such excitations will probably be detected eventually, but the present theoretical description of their energy and coupling (both in this work and in the Appendix of Ref. 8) are only rough estimates. We are also hopeful that losses to distinct trapped waves near ω_3 may some day be resolved. However, the energy resolution of the ZnO experiments is presently 15 meV,[8] which must (and probably can[34]) be improved by an order of magnitude.

Since the detection of these trapped modes would be an important confirmation of our theory we conclude by summarizing their parameter dependence. They lie above ω_T, just below ω_L. They owe their existence in our model to the finite layer of carriers, but neither their location nor external coupling depend sensitively on the key parameter N, the number of electrons per area in the surface layer. This point is illustrated in Fig. 3 where we show the spectral function

$$B=\mathrm{Im}[-\lambda(\vec{Q},\omega)] \tag{20}$$

along the line

$$Q=(k_i\sin\theta_i)\left[\frac{\hbar\omega}{2E_i}\right], \tag{21}$$

where k_i, E_i, and θ_i are the incident wave vector, energy, and angle of 10-V electrons specularly scattering at $55°=\theta_i$ from the surface. Note that since these Q's are well beyond ω/c, where c is the speed of light, retardation effects should not affect the modes seen in EELS; see also Fig. 2. The use of Eq. (21) partially accounts for the effect of the kinematic factor in (5). A complete calculation for EELS would average (5) over the experimental angle and energy resolution functions. This would enhance the low-ω structure in Fig. 3, since the kinematic factor varies roughly as ω^{-3}, but would also, with present resolution limits, wash out the individual peaks near ω_L. Hence to

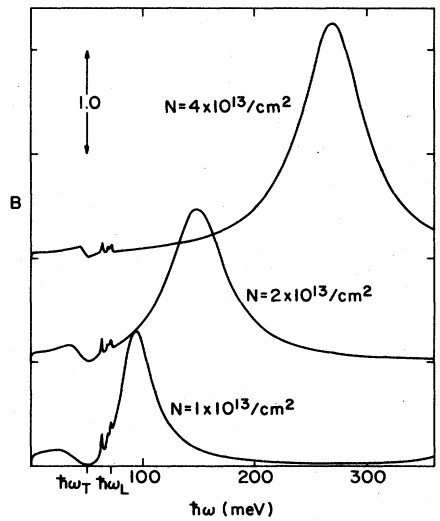

FIG. 3. Spectral weight function B of Eqs. (20) and (21) versus energy. Results for three separate choices of N are shown, each separated vertically by one unit for clarity.

show what one is seeking we have plotted just B, which includes only the broadening due to the decay rates $\hbar\gamma=1$ meV and $\hbar/\tau=40$ meV, as estimated in the Appendix. The $n=1$ and 2 modes are resolved and the remainder produce a third peak. Although the ω_2 loss moves dramatically with N (and hence is a sensitive measure of N), the losses near ω_L are scarcely affected. Moving into off-specular directions should also not shift the extra mode locations since they have little dependence on Q.

ACKNOWLEDGMENT

This work was supported in part by the National Science Foundation (NSF) through Grant No. DMR 81-15705.

APPENDIX

Here we describe the choice of parameter values used in our models. Some are taken as fixed, in particular those adopted from Gersten:[11,12] $m^*/m=0.25$, $\hbar\omega_T=50.7$ meV, $\hbar\omega_L=71.7$ meV, and $\epsilon_\infty=4.0$. Others are estimated from different experiments:[5–8,35,36] $\hbar\gamma=1$ meV and $\hbar/\tau=40$ meV. The latter comes from a mobility estimate of $\mu\sim100$ cm^2/V sec for electrons in the accumulation layer.[8] We note in passing that Gersten's method of inserting damping is rather different from ours since it is appended after the modes have been found, whereas ours enters at the first stages, (1) and (2).

The remaining parameters all depend on $N=dn_0$. We view N as experimentally set, although it has not yet been simultaneously measured with EELS—only μN is reported.[5–8] This is no problem since the sensitive dependence of ω_2 on N (see Fig. 3) makes it simple to fit. We still need to separate N into d and n_0, which we accomplish by the variational calculation outlined below. Given n_0, the spatial dispersion parameter is calculated from $\beta=\hbar k_F/(\sqrt{3}m^*)$ where $k_F=(3\pi^2 n_0)^{1/3}$.

Our variational calculation of d is analogous to Gersten's estimate[12] of his parameter α^{-1}, except we do not acknowledge size quantization. The electronic energy of the layer is written for a given N as $E(d)=E_K+E_P$. Here the kinetic energy E_K is approximated by the free-electron energy of a uniform slab of area A and thickness d:

$$E_K=NA(\tfrac{3}{5}\epsilon_F)=\frac{3\hbar^2}{10m^*}(3\pi^2N/d)^{2/3}NA\ , \tag{A1}$$

while the potential energy E_P is represented by the electrostatic energy

$$E_P=\frac{A}{2}\int_0^d dx\,\rho(x)\Phi_0(x)\ , \tag{A2}$$

where

$$\nabla^2\Phi_0=-\frac{4\pi}{\epsilon_0}\rho \tag{A3}$$

with $\epsilon_0/\epsilon_\infty=\omega_L^2/\omega_T^2=2.0$ for ZnO.[12] The charge density in equilibrium is assumed to be

$$\rho(x)=N\,|\,e\,|\,[\delta(x)-\Theta(x)\Theta(d-x)/d]\ , \tag{A4}$$

which represents a localized layer of ions and a (uniform) diffuse layer of electrons. With (A4), one can easily solve (A3) and evaluate the integral (A2) to obtain

$$E_P=\frac{2\pi}{3\epsilon_0}N^2e^2Ad\ . \tag{A5}$$

Then we find that the value of d that minimizes $E(d)$ is

$$d=(82.1\ \text{Å})\left[\frac{10^{10}/\text{cm}^2}{N}\right]^{1/5}. \tag{A6}$$

Hence given N we can easily calculate d and $n_0=N/d$.

---

*Present address: NL MWD/National Lead Industries Inc., P.O. Box 60070, Houston, Texas 77205.

[1]W. L. Schaich, Surf. Sci. **122**, 175 (1982).
[2]R. Matz and H. Luth, Phys. Rev. Lett. **46**, 500 (1981).
[3]H. Luth, Festkoerperprobleme **21**, 117 (1981).
[4]M. Liehr and H. Luth, J. Vac. Sci. Technol. **16**, 1200 (1979).
[5]Y. Goldstein, A. Many, I. Wagner, and J. Gersten, Surf. Sci. **98**, 599 (1980).
[6]A. Many, I. Wagner, A. Rosenthal, J. I. Gersten, and Y. Goldstein, Phys. Rev. Lett. **46**, 1648 (1981).
[7]A. Many, J. I. Gersten, I. Wagner, A. Rosenthal, and Y. Goldstein, Surf. Sci. **113**, 355 (1982).
[8]J. I. Gersten, I. Wagner, A. Rosenthal, Y. Goldstein, A. Many, and R. E. Kirby, Phys. Rev. B **29**, 2458 (2984).
[9]See the conference reports in the following volumes of Surf. Sci.: **58**, 1976; **73**, 1978; **98**, 1980; **113**, 1982; and **142**, 1984. Also see review papers in *Surface Polaritons,* edited by V. M. Agranovich and D. L. Mills (North-Holland, New York, 1982).
[10]T. Ando, A. B. Fowler, and F. Stern, Rev. Mod. Phys. **54**, 437 (1982).
[11]J. I. Gersten, Surf. Sci. **92**, 579 (1980).
[12]J. I. Gersten, Surf. Sci. **97**, 206 (1980).
[13]W. L. Schaich and C. Schwartz, Phys. Rev. B **25**, 7365 (1982).
[14]W. L. Schaich, Phys. Rev. B **24**, 686 (1981).
[15]Bulk modes for our models produce no external effects.
[16]R. H. Ritchie, Phys. Rev. **106**, 874 (1957).
[17]R. A. Ferrell, Phys. Rev. **111**, 1214 (1958).
[18]F. Stern, Phys. Rev. Lett. **18**, 546 (1967).
[19]A. L. Fetter, Ann. Phys. **81**, 367 (1973).
[20]A. D. Karsono and D. R. Tilley, J. Phys. C **10**, 2132 (1977).
[21]A. A. Lucas and M. Sunjic, Prog. Surf. Sci. **2**, 75 (1972).
[22]F. J. Crowne, Phys. Rev. B **27**, 3201 (1983).
[23]S. Das Sarma, J. J. Quinn, and A. Eguiluz, Solid State Commun. **38**, 731 (1981).
[24]J. J. Quinn, A. Eguiluz, R. F. Wallis, and S. Das Sarma, J. Vac. Sci. Technol. **19**, 402 (1981).
[25]M. Nakayama, J. Phys. Soc. Jpn. **36**, 393 (1974).

[26]C. Tannous and A. Caille, Phys. Status Solidi B **97**, K77 (1980).
[27]R. T. Holm and E. D. Palik, Phys. Rev. B **17**, 2673 (1978).
[28]C. Schwartz and W. L. Schaich, J. Phys. C **17**, 537 (1984).
[29]C. Schwartz and W. L. Schaich, Phys. Rev. B **26**, 7008 (1982).
[30]S. J. Allen, Jr., D. C. Tsui, and B. Vinter, Solid State Commun. **20**, 425 (1976).
[31]D. A. Dahl and L. J. Sham, Phys. Rev. B **16**, 651 (1977).
[32]A. Eguiluz and A. A. Maradudin Ann. Phys. (N.Y.) **113**, 27 (1978).
[33]W. P. Chen, Y. J. Chen, and E. Burstein, Surf. Sci. **58**, 263 (1976).
[34]L. Kesmodel, J. Vac. Sci. Technol. A **1**, 1456 (1983).
[35]H. Ibach, Phys. Rev. Lett. **24**, 1416 (1970); J. Vac. Sci. Technol. **9**, 713 (1972).
[36]E. C. Heltemes and H. L. Swinney, J. Appl. Phys. **38**, 2387 (1967).